Spatial Dopant Profiles For Transverse-Mode Selection in Multi-Mode Waveguides

T.Bhutta, J.I.Mackenzie, and D.P.Shepherd

Optoelectronics Research Centre, University of Southampton

Highfield, Southampton SO17 1BJ, UK

R.J.Beach

Maxios Laser Corporation, 4749-A Bennett Drive

Livermore CA 94550, USA

We theoretically investigate the effect of the spatial distribution of the active-ion concentration in multi-mode step-index waveguides on transverse-mode selection for continuous-wave laser operation. It is found that uniform doping of a central portion of up to 60% of the full waveguide core-width is very effective in selecting fundamental-mode operation, even under highly saturated, high-power conditions. Profiling the dopant distribution to match that of the particular mode desired is also found to be effective, especially if it is the saturated inversion profile that is matched to the shape of the mode.

OCIS codes:

140.3430 140.3460 130.2790

1. INTRODUCTION

There is a growing interest in the use of guided-wave geometries for high-power laser operation, both in fibre[1,2] and planar formats[3,4]. The use of high-power diode pump lasers requires multi-mode waveguides for the confinement of these non-diffraction-limited light sources, but most applications require fundamental-mode laser operation. In optical fibres this can be achieved by using cladding-pumping techniques[5], such that the pump and laser signals are guided by different, but spatially overlapping, waveguides. However, such a technique is hard to apply to the planar geometry because of the associated large increase in length required to absorb the pump. Even in a fibre geometry, energy storage, power handling, and avoidance of non-linear effects can lead to a desire for large-mode-area[6], and hence multi-mode, waveguides. One technique that has been used to select fundamental-mode operation from multi-mode waveguides is to limit the doping region to a central portion of the waveguide to give a preferential overlap with the fundamental mode[6,7]. Here, we theoretically investigate how tailoring the doping profile in this way can lead to the required modal discrimination in continuous-wave lasers, and we investigate the effects of gain saturation, which itself varies spatially, on this selectivity. We show that, even under highly saturated, high-power conditions, fundamental-mode operation can be robustly selected and compare our results with reported experimental data. It is also found that, if desired, individual high-order modes can be preferentially selected through tailoring of the dopant profile, and that higher modal discrimination can be obtained by accounting for the change in the gain distribution due to saturation by the lasing mode.

The model presented at the beginning of this paper is based around the analysis of Risk[8] and can be applied to many different situations including planar, fibre and bulk geometries. However, we will then concentrate on planar waveguides with doping profiles that vary in just one-dimension. This simplest of cases corresponds directly to our work on double-clad YAG waveguide lasers[3,7,9], and also brings out features that are common to many geometries.

2. THEORY

Let us assume a quasi-three-level laser transition and an energy level diagram and population densities as defined by Risk[8], see figure 1. We will continue to follow the analysis of Risk[8], but modify it to allow for a transverse spatial variation in the doping concentration. We also assume a uniform pump distribution due to the highly multi-mode nature of the waveguide and high-power diode pump source. The rate equation for the population inversion density, $\Delta N(x,y,z)$, assuming negligible ground state depletion, is then,

$$\frac{d\Delta N(x,y,z)}{dt} = fRd(x,y,z) - \frac{\Delta N(x,y,z) + n_1^0 d(x,y,z)}{\tau} - \frac{fc\sigma\Delta N(x,yz)}{n}\Phi\phi(x,y,z) = 0 \qquad \ldots(1)$$

where $f=f_1+f_2$ (see figure 1), τ is the lifetime of the upper laser-level manifold, c is the speed of light, and σ is the gain cross-section. The rate at which ions are pumped into the upper laser manifold is given by $R=P_a/h\upsilon_p$, where P_a is the absorbed pump power and υ_p is the pump frequency. The unpumped population density in the lower laser

level is given by $n_1^0 d(x,y,z)$, where n_1^0 is the total population in the unpumped lower laser level and $d(x,y,z)$ is the dopant profile normalised such that,

$$\iiint d(x,y,z)dV = 1 \qquad \ldots(2)$$

The total number of laser photons in the cavity is given by $\Phi = 2nlP_l/chv_l$, where P_l is the one-directional intracavity laser power in the waveguide, n is the refractive index, l is the length of the cavity, and v_l is the laser frequency. The spatial distribution of the photons, $\phi(x,y,z)$, is normalised such that,

$$\iiint \phi(x,y,z)dV = 1 \qquad \ldots(3)$$

From equation (1) we can see that below threshold (Φ=0) the inversion has the same spatial distribution as the doping and the ground state population (which does not change in shape due to our assumption of negligible ground state depletion). As shown by Risk[8], at threshold and above the inversion averaged over the laser-mode profile becomes clamped at the threshold value such that,

$$\iiint \Delta N(x,y,z)\phi(x,y,z)dV = \frac{L+T}{2\sigma l} \qquad \ldots(4)$$

where L is the round-trip loss and T is the transmission of the output coupler. However, the spatial distribution of the inversion above threshold will change due to saturation by the lasing photons. From equation (1) it can be seen that above threshold,

$$\Delta N(x,y,z) = \frac{\eta f R d(x,y,z) - n_1^0 d(x,y,z)}{1 + \frac{c\sigma\tau}{n} f\Phi\phi(x,y,z)} \qquad \ldots(5)$$

We can combine equations (4) and (5) to give the population inversion distribution expressed only in terms of the losses and the laser power,

$$\Delta N(x,y,z) = \frac{d(x,y,z)(L+T)}{2\sigma l\left(1+S\phi(x,y,z)\right)\iiint \frac{d(x,y,z)\phi(x,y,z)}{1+S\phi(x,y,z)}dV} \qquad \ldots(6)$$

where $S=2fIP_l\sigma\tau/h\upsilon_l$ gives a measure of the degree of saturation caused by the intracavity laser power. The gain exponent, G_p, for a particular mode with spatial distribution ϕ_p, with a population inversion saturated by a lasing mode with spatial distribution ϕ, is then given by,

$$G_p = 2\sigma l \iiint \Delta N(x,y,z)\phi_p(x,y,z)dV \qquad \ldots(7)$$

Equations (6) and (7) can now be combined to give the gain for each mode, ϕ_p, relative to the lasing mode, ϕ,

$$G_{rel} = \frac{G_p}{L+T} = \iiint \frac{d(x,y,z)\phi_p}{\left(1+S\phi(x,y,z)\right)\left[\iiint \frac{d(x,y,z)\phi(x,y,z)}{1+S\phi(x,y,z)}dV\right]}dV \qquad \ldots(8)$$

Equation (8) can be evaluated to give the relative gain for each waveguide mode for a given dopant distribution, saturating distribution, and saturating power. It should be noted that, as a direct result of the uniform pumping distribution in a highly multi-mode waveguide, this selectivity is independent of n_1^0, and thus the same results will be obtained for 4-level or quasi-3-level lasers.

3. ONE-DIMENSIONAL STEP-FUNCTION DOPING DISTRIBUTION

Experimental work in planar[3,7,9], fibre[2,6] and bulk lasers[10] has used step-function dopant distributions restricted to a central region of the allowed modes, as this is relatively easy in terms of fabrication. Figure 2 shows an example of a one-dimensional step-function doping profile together with the three lowest-order waveguide modes of a highly multimode, step-index waveguide of depth, D. This one-dimensional example is taken as the simplest case to initially investigate. We now make the assumption that the modes are far from cut-off and so are fully confined within the core. The normalised spatial distribution of photons (equation (3)) for the even and odd modes is then given by[11],

$$\phi_{even}(x,y,z) = \frac{2}{WDL}\cos^2\left(\frac{(m+1)\pi x}{D}\right) \qquad \ldots(9a)$$

$$\phi_{odd}(x,y,z) = \frac{2}{WDL}\sin^2\left(\frac{(m+1)\pi x}{D}\right) \qquad \ldots(9b)$$

where m is the mode number (m=0,2,4... for the even modes and m=1,3,5... for the odd modes), L is the length of the guide, and W is the width of the guide.

It can be visualised from figure 2 that doping a fraction, r/D, of the core can lead to a preferential gain for the fundamental mode. Applying equation (9) and the step-function doping of figure 2 to equation (8) allows us to calculate the relative gain for each of the waveguide modes in this situation. Figure 3 shows the results of this calculation for the ten lowest-order modes, and how it varies with doping fraction, for the case of no signal saturation (i.e. at lasing threshold). For very small doped-fractions the gain for all the even modes becomes equal as all these modes have a central peak in their intensity profiles, whereas the gain for the odd modes tends to zero as these modes have zero intensity at the centre of the core. The gain for all the modes becomes equal for a fully doped core, showing that a normal multi-mode waveguide will indeed suffer from multi-mode laser output. For intermediate doped fractions, there is a clear gain advantage for the fundamental mode, implying that this mode will lase first.

However, once lasing occurs, the fundamental mode will start to saturate the inversion, altering its spatial profile in a way that may change the mode selectivity from that shown in figure 3. The saturation behaviour for three different doped fractions, due to saturation by the fundamental mode is shown in figure 4. It can be seen that the change in shape of the inversion profile is much smaller for the smaller doping fractions. It is also interesting to note that very little change occurs in the saturation profile once the intensity of the laser beam reaches several times the saturation intensity.

Figure 5 shows the relative gain for the ten lowest-order waveguide modes under highly saturated conditions (I/I_{sat}=100). It can be seen that, as expected, heavy

saturation can lead to the gain for the high-order modes becoming larger than that for the fundamental mode. It appears that it is always the lowest-order odd mode (m=1) that is the first higher-order mode to oscillate. However, we can also see that there is still a window for doping fractions below 0.6 with a clear gain advantage for the fundamental mode. The result of figure 5 also remains virtually unchanged for even higher lasing powers, due to the unchanging inversion profile at high saturation levels. Figure 6 shows a plot of the doping fraction at which the gain for the m=1 mode becomes equal to the m=0 mode against the intracavity lasing intensity. Once again we can see that the fraction is virtually unchanging once the intensity is greater than a few times the saturation intensity. Thus, in practice, taking into consideration a desire to not increase the pump absorption length too much, a doping fraction of approximately 0.5 would appear to be a good choice for robust fundamental mode selection at high laser powers. It should be noted that once a higher-order mode starts to oscillate equation 8 is no longer valid, as this new mode will also contribute to the saturation of the gain. However, in this work, we are only interested in the regime where a single transverse mode is oscillating.

There are some practical limitations on the use of this method. Firstly, the active-ion doping normally brings with it a small change in refractive index. Therefore, at a certain doping width, it will create its own waveguide, rather than merely modifying the properties of the highly multi-mode guide, and the mode-selecting properties will be lost. Secondly, for high-power operation the thermal loading of the doped region will also have an effect upon its refractive index, which must be taken into consideration. The closest experimental work to the structure modelled here is that of diode-pumped double-clad YAG planar waveguides, which

have been operated at high power (>10W) for Nd, Yb and Tm dopants[3,7,9]. In those experiments doping fractions up to 0.67 were found to give fundamental mode operation. The reason for this better-than-expected performance may be due to our initial assumption of an unchanging ground-state population. In reality, the regions that are heavily saturated by the laser signal would have a correspondingly increased pump absorption due to the increased population in the ground level. This would then act against the effects described previously and aid fundamental-mode selection. Thus it appears that our model may be a worst-case limit, which can be seen as a useful design feature. We have also assumed that the losses for each mode are the same, which may not necessarily be the case.

4. ONE-DIMENSIONAL PROFILED DOPING DISTRIBUTIONS

If the fabrication technique allows, then higher selectivity can be obtained with a more sophisticated doping profile. For instance, if we make a doping profile proportional to the square of the fundamental mode profile we find that the final saturated profile is still Guassian-like, as shown in figure 7. Consequently, the mode selectivity of such a profile is very high, even for full doping fractions, as shown in figure 8.

It should also be noted that it is not just the fundamental mode that can be selected. For instance, by setting the doping profile to be the square of the m=9 mode profile, similar calculations show that we can expect laser operation to occur robustly on this single higher-order mode.

5. OTHER GEOMETRIES

The theory developed here, as expressed in equation (8), can certainly also be used to analyse modal-discrimination of two-dimensional doping distributions. Practical examples of this include the large-mode-area fibre[2,6] and bulk lasers with composite rods[10]. However, the selectivity in a fibre will be compromised by the fact that, due to bending, there is always a certain degree of coupling between the propagation modes. For the case of a bulk laser, it should be noted that the selectivity is between the modes of the resonator, rather than the propagation modes of a waveguide.

6. SUMMARY

A rate-equation approach has been used to find the transverse-mode discrimination that can be obtained in a continuous-wave laser by spatially varying the active-ion dopant distribution. For a highly multi-mode waveguide pumped by a high-power diode-bar, which allows the assumption of a uniform pump distribution, we find that restricting the doping to a central portion (<60%) of the core can be used to robustly select fundamental-mode operation, even for highly saturated, high-power operation. For higher doping fractions, multi-mode operation will occur. We also find that profiling the dopant distribution such that the saturated inversion profile matches the shape of the particular transverse-mode desired, also gives a high modal-discrimination, whether it is for the fundamental mode or a higher-order mode.

ACKNOWLEDGEMENTS

The authors would like to acknowledge support from UK EPSRC grant GR/M98449/01. Tajamal Bhutta acknowledges support from an EPSRC studentship and from Onyx Optics Inc..

References

1. V.Dominic, S.MacCormack, R.Waarts, S.Sanders, S.Bicknese, R.Dohle, E.Wolak, P.S.Yeh and E.Zucker, "110W fibre laser," Electron. Lett., **35**, 1158-1160 (1999).
2. J.A.Alvarez-Chavez, H.L.Ferhaus, J.Nilsson, P.W.Turner, W.A.Clarkson, D.J.Richardson, "High-energy, high-power, ytterbium-doped Q-switched fiber laser," Opt. Lett., **25**, 37-39 (2000).
3. R.J.Beach, S.C.Mitchell, H.E.Meissner, O.R.Meissner, W.F.Krupke, J.M.McMahon, W.J.Bennett , and D.P.Shepherd, "Continuous-wave and passively Q-switched cladding-pumped planar waveguide devices," Opt. Lett. **26**, 881-883 (2001).
4. J.R.Lee, G.J.Friel, H.J.Baker, G.J.Hilton, and D.R.Hall, "A Nd:YAG planar waveguide laser operated at 121W output with face pumping by diode bars, and its use as a power amplifier," in *Advanced Solid State Lasers Meeting*, Technical Digest (Optical Society of America, Washington DC, 2001) paper TuC3-1.
5. E.Snitzer, H.Po, F.Hakimi, R.Tumminelli, and B.C.McCollum, "Double-clad, offset core Nd fiber laser," in *Conference On Optical Fiber Communication*, Technical Digest (Optical Society of America, Washington DC, 1988) paper PD5.
6. H.L.Offerhaus, N.G.Broderick, D.J.Richardson, R.Sammut, J.Caplen, and L.Dong, "High-energy single-transverse-mode Q-switched fiber laser based on a multi-mode large-mode-area erbium-doped fiber," Opt. Lett. **23**, 1683-1685 (1998).

7. C.L.Bonner, T.Bhutta, D.P.Shepherd, and A.C.Tropper, "Double-clad structures and proximity coupling for diode-bar-pumped planar waveguide lasers," IEEE J. Quantum Electron., **36**, 236-242 (2000).
8. W.P.Risk, "Modeling of longitudinally pumped solid-state lasers exhibiting reabsorption losses," J. Opt. Soc. Am. B, **5**, 1412-1423 (1998).
9. J.I.Mackenzie, S.C.Mitchell, R.J.Beach, H.E.Meissner, and D.P.Shepherd, "15W diode-side-pumped Tm:YAG waveguide laser at 2μm," Electr. Lett. **37**, 898-899 (2001).
10. A.Lucianetti, R.Weber, W.Hodel, H.P.Weber, A.Papashvili,V.A.Konyushkin, and T.T.Basiev, "Beam-quality improvement of a passively Q-switched Nd:YAG laser with a core-doped rod," Appl. Opt. **38**, 1777-1783 (1999).
11. D.L.Lee, *Electromagnetic Principles of Integrated Optics* (John Wiley and Sons, New York, 1986), ch.4.

Figure Captions

Figure 1 Energy level diagram where $N_{0\text{-}3}$ are the population densities of the particular Stark levels involved such that $N_2=f_2N_U$ and $N_1=f_1N_L$, where N_U and N_L are the population densities of the upper and lower laser level manifolds, and $f_{1,2}$ are the fractional occupancies.

Figure 2 Step-function doping of the central region of the core, and the three lowest-order propagation modes of the highly multi-mode waveguide.

Figure 3 Relative gain for the ten lowest-order modes against doping fraction for $I/I_{sat}=0$, where I is the intracavity lasing intensity and $I_{sat}=h\nu/\sigma\tau$ is the saturation intensity.

Figure 4 Spatial distribution of the inversion for various levels of saturation by the fundamental mode, for doping fractions (a) 1, (b) 0.6, and (c) 0.3.

Figure 5 Relative gain for the ten lowest-order modes against doping fraction, for a heavily saturated gain region.

Figure 6 Graph of doping fraction at which high-order-mode oscillation occurs against I/I_{sat}.

Figure 7 Spatial distribution of the inversion for various levels of saturation by the fundamental mode, for an original doping profile that is the square of the fundamental-mode profile.

Figure 8 Relative gain for the ten lowest-order modes against doping fraction when matching the heavily saturated doping profile to the fundamental-mode profile.

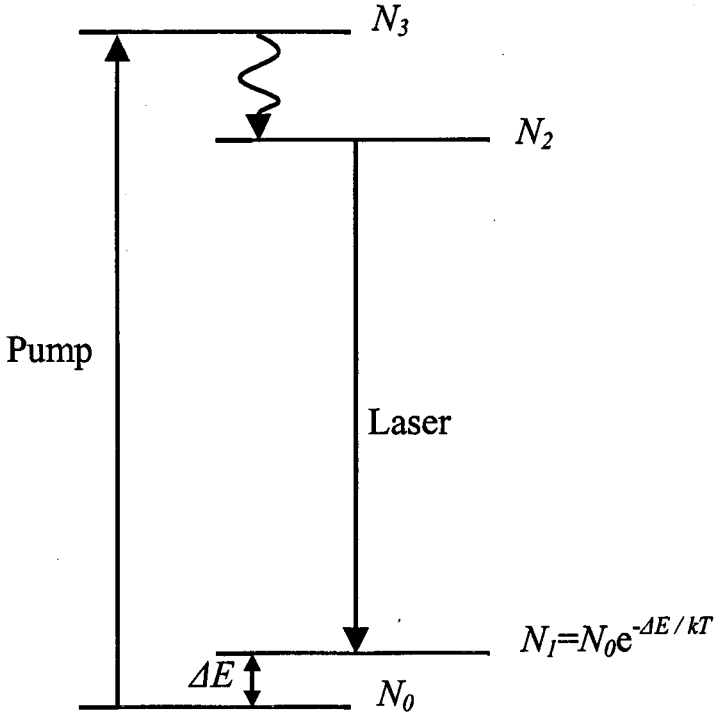

Figure 1

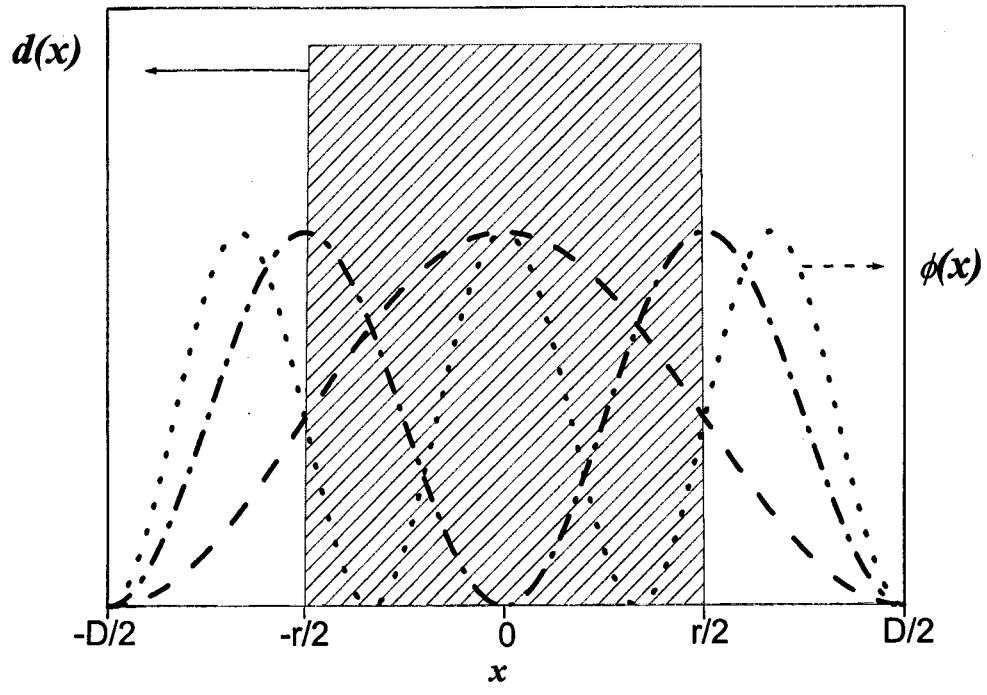

Figure 2

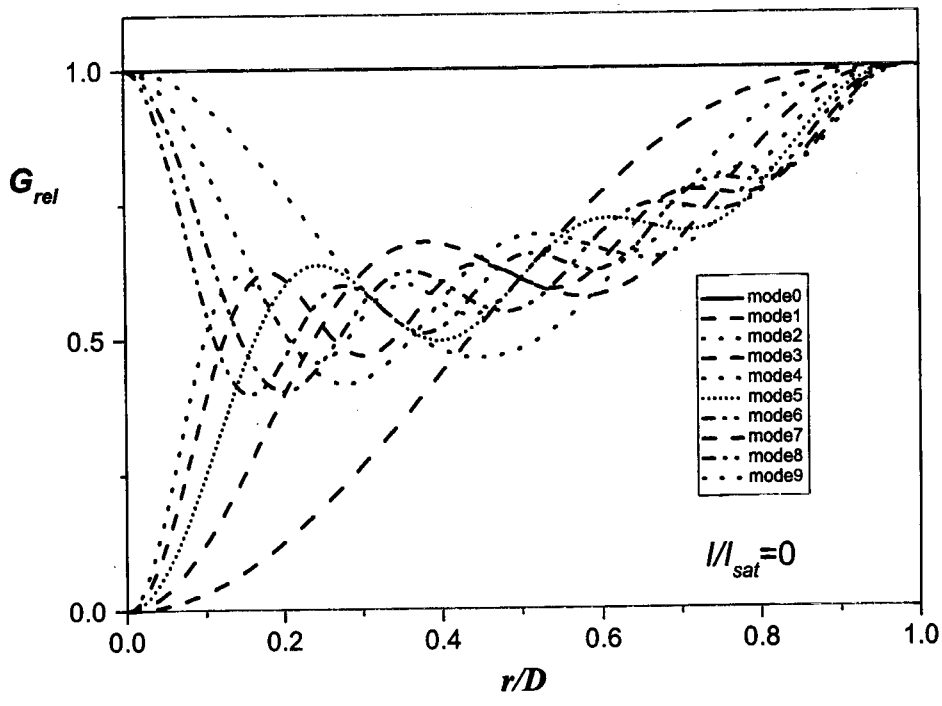
1.0
0.5
0.0
G_{rel}
0.0
0.2
0.4
0.6
0.8
1.0
r/D
mode0
mode1
mode2
mode3
mode4
mode5
mode6
mode7
mode8
mode9
I/I_{sat}=0

Figure 3

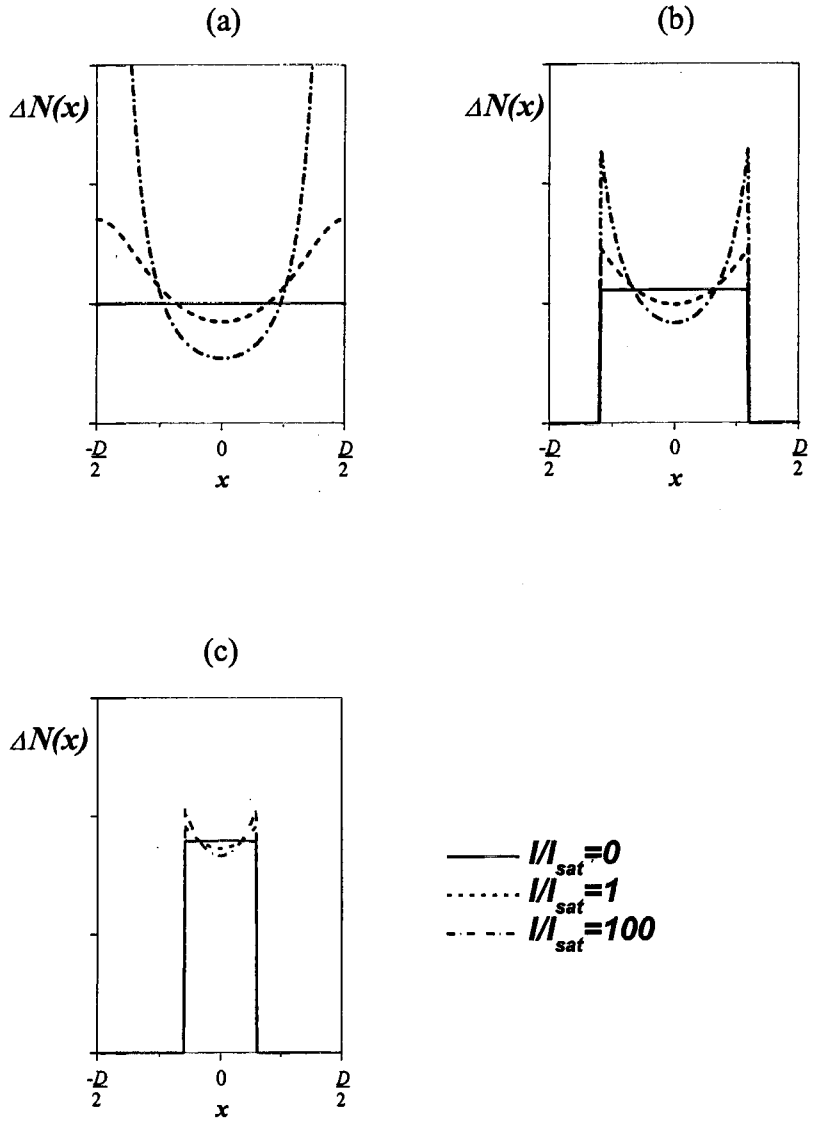
(a)
(b)
(c)
ΔN(x)
ΔN(x)
ΔN(x)
-D/2
0
D/2
x
-D/2
0
D/2
x
-D/2
0
D/2
x
I/I_sat=0
I/I_sat=1
I/I_sat=100

Figure 4

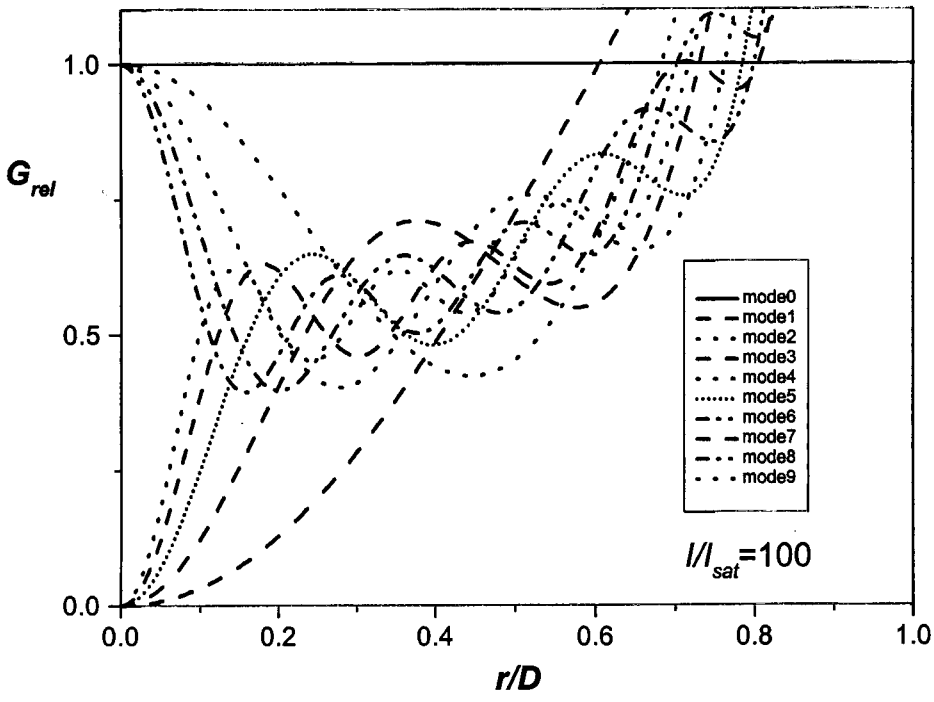
1.0
0.5
0.0
G_{rel}
0.0
0.2
0.4
0.6
0.8
1.0
r/D
mode0
mode1
mode2
mode3
mode4
mode5
mode6
mode7
mode8
mode9
I/I_{sat}=100

Figure 5

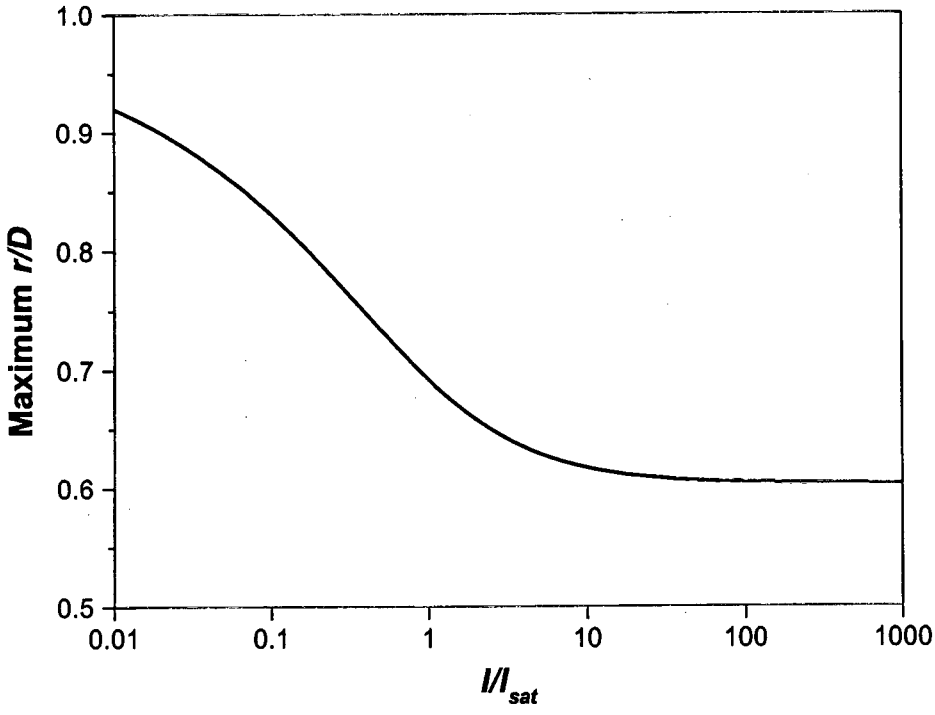

Figure 6

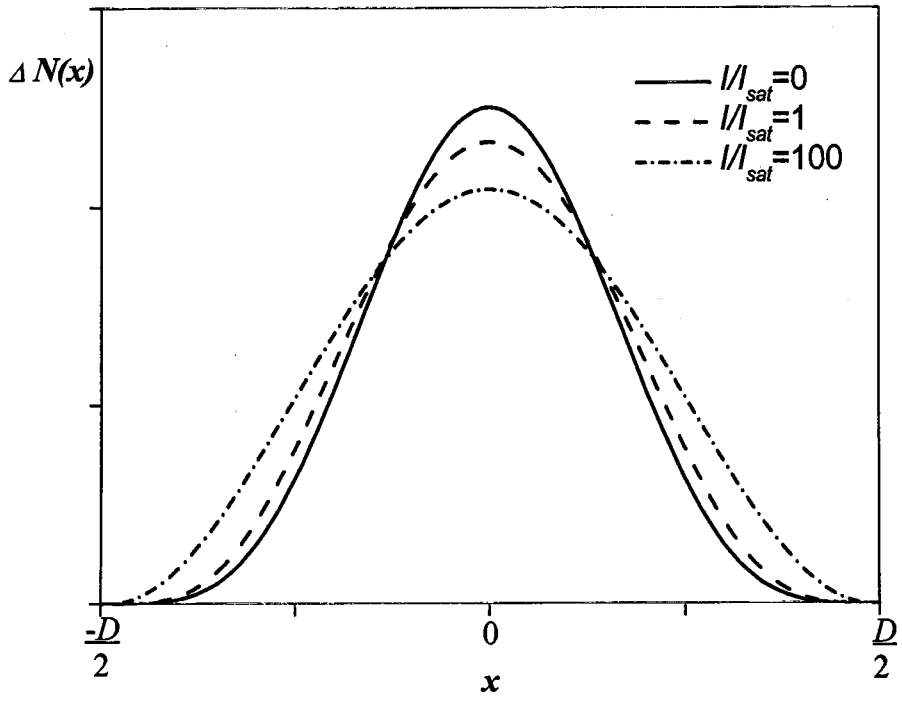

Figure 7

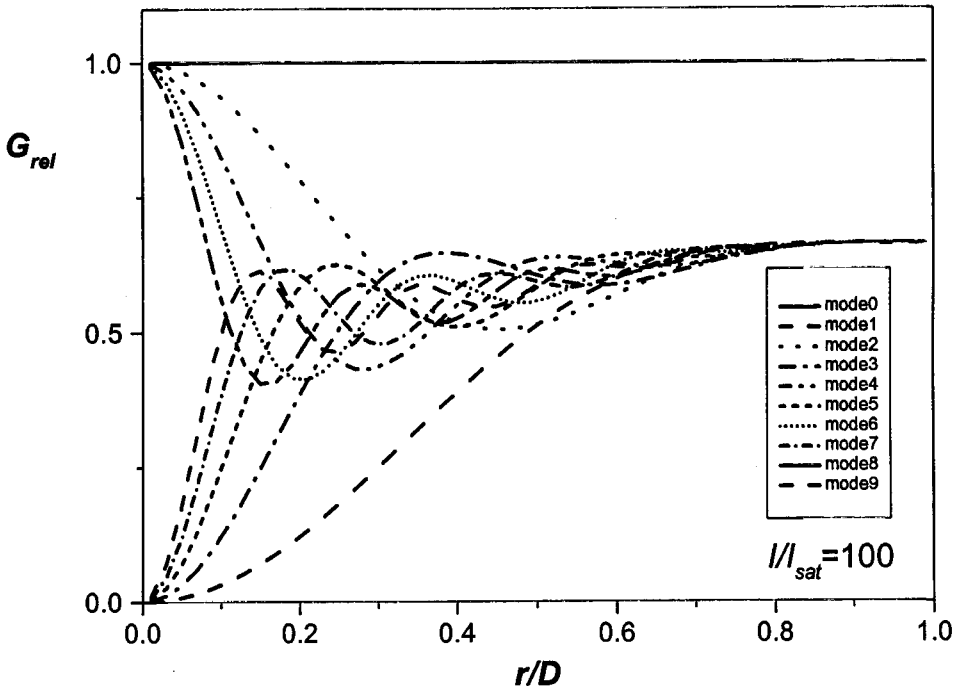
1.0
0.5
0.0
G_{rel}
0.0
0.2
0.4
0.6
0.8
1.0
r/D
mode0
mode1
mode2
mode3
mode4
mode5
mode6
mode7
mode8
mode9
I/I_{sat}=100

Figure 8